<center>**SI Appendix**</center>

SI Appendix includes:

Details about numerical calculations

Simulations on the He$^+$ ions injection

Figures S1-S12

Supplementary Video captions 1-6

Details about numerical calculations

We model and numerically solve our system as the Mott resistor network model as schematize in Fig. S7a. A load resistance R_{load} is making a voltage divisor circuit with a resistor tensor network. Each site of our grid of size $L \times W$ is represented by 4 resistors of 3 possible values $R_{cm}^{VO_2}$, $R_{cm}^{V_5O_9}$, and $R_{MI}^{VO_2}$ (*cm* is short form of correlated metal, while *MI* is Mott Insulator). The system is initially fully insulator, *i.e.* all resistors are equal to $R_{MI}^{VO_2}$. For a finite amount of time t_{pulse} a constant voltage V is applied in order to obtain a voltage of the system:

$$V_S = \frac{R_S}{R_S + R_{\text{load}}} \tag{1}$$

where R_S denoted the total resistance of the resistors network. After the pulse the system relax and then can be applied or not another pulse. At each cycle of our simulations the entire network of resistors is updated following the probabilities:

The probability to switch from a metallic to an insulating state of VO$_2$:

<center>1</center>

$$P_{CM_{VO_2} \to MI_{VO_2}} = e^{\frac{-(E_B^{VO_2} - E_{cm}^{VO_2})}{KT}} \tag{2}$$

The probability to switch from an insulating to a metallic state of VO_2:

$$P_{MI_{VO_2} \to CM_{VO_2}} = e^{\frac{-(E_B^{VO_2} - E_{MI}^{VO_2})}{KT}} \tag{3}$$

The probability to switch from an insulating state of VO_2 to a metallic state of V_5O_9:

$$P_{MI_{VO_2} \to CM_{V_5O_9}} = e^{\frac{-(E_B^{V_5O_9} - E_{MI}^{VO_2} - \Delta V)}{KT}} \tag{4}$$

The probability to switch from a metallic state of V_5O_9 to either state of VO_2:

$$P_{CM_{V_5O_9} \to VO_2} = e^{\frac{-(E_B^{V_5O_9} - E_{cm}^{V_5O_9})}{KT}} \tag{5}$$

Then the probability to be in a metallic state of VO_2 is: $\dfrac{e^{\frac{-E_{cm}^{VO2}}{KT}}}{e^{\frac{-E_{cm}^{VO2}}{KT}} + e^{\frac{-E_{MI}^{VO2}}{KT}}}$.

$E_{MI}^{VO_2}$, $E_{cm}^{VO_2}$ and $E_B^{VO_2}$, *i.e.* the energy of the insulating and metallic state of VO_2 and the energy barrier between these 2 states, are computed in the same way of (*1*) as sketched in Fig. S7c and reported in Fig. S7d, and far away from the first order transition of VO_2 are kept constant, as done in (*2*). Instead, $E_{cm}^{V_5O_9}$ and $E_B^{V_5O_9}$ are respectively the energy of the metallic state of V_5O_9 and the energy barrier toward a state of VO_2. As shown in Fig. S7d, the values of these parameters are renormalized in respect of $E_{MI}^{VO_2}$ in order to maintain a constant difference $E_B^{V_5O_9} - E_{MI}^{VO_2}$ and $E_B^{V_5O_9} - E_{cm}^{V_5O_9}$ due to the physical interpretation of this transition. Indeed, the chemical barrier needed by the oxygens to leave the molecules is evaluated as constant in temperature. K is the Boltzmann constant, ΔV is the local voltage drop of the site and T is the local temperature on the site. As done in (*1*), the temperature is updated at each

cycle by the following formula:

$$T_{ij} = T_{subs} + \frac{V^2}{C_v R_{ij}} + 4T_{ij} - k_h \sum_{<ik>}^{firstneighbor} T_{ik} \qquad (6)$$

Where the indices i and j denotes the coordinates of the site in the network, C_v the specific heat of the system, k_h the thermal conductivity and $\sum_{<ik>}^{firstneighbor}$ denotes the summation over the first neighboring sites around the one with coordinates ij.

Simulations on the He$^+$ ions injection.

V_5O_9 can be thought of as an O-deficient VO_2 as has been shown in the main text. This realization leads us to the speculative possibility that we could prepare the VO_2 spatially to induce the current or E-field motivated transition directly. For practical reasons it would be of great advantage to locate where the filaments would be likely to form and the density of filaments to be written. Furthermore, it is possible that a spatially prepared VO_2 with O deficiencies would present a lower threshold for the onset of V_5O_9 metallic state resulting in a designed pattern of filaments and lower power consumption. With this in mind, we have simulated such a structure applying a finely focused He$^+$ ion beam. We have access to such a beam with radius ~1 nm which has been used to write disorder in the high Tc superconductor $YBa_2Cu_3O_7$ (*3*). In Fig. S12a we show the calculated ion tracks for a 35 keV He$^+$ ion incident on a film of VO_2 using the program SRIM. In this figure we show the ion tracks for 5000 ions incident normal to a VO_2 film of 1500 Å thickness (the thickness of the samples studied in the main text). With a finely focused incident beam, the ion scattering causes the beam to broaden to ~200-

250 A fwhm. Even more interesting is a plot of the resultant displacement shown in Fig. S12b. The beam results in a narrow track of displacements throughout the film. It is this result which tempts us to expect that this technology will afford us substantial control over the creation of conducting filaments in the VO_2.
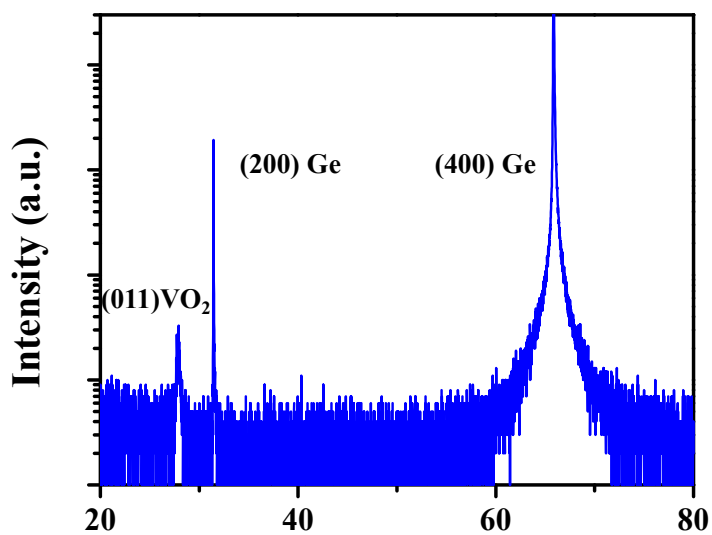
Figures and Captions

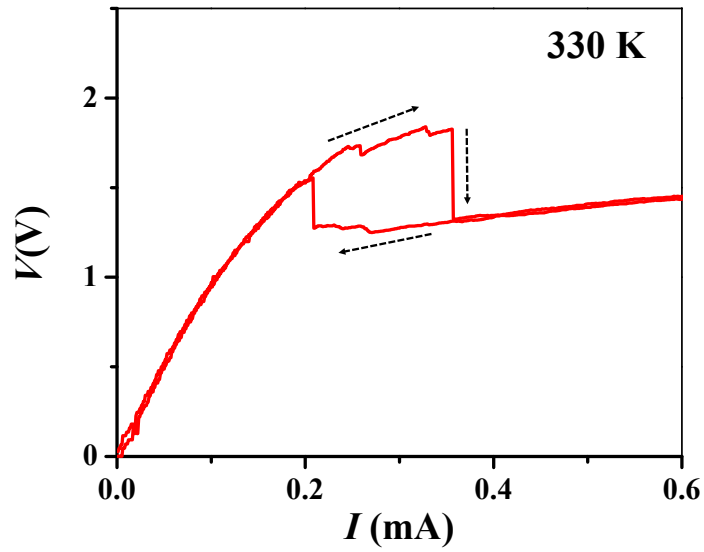**Fig. S1. Room-temperature XRD scans for vanadium oxide films on (100) Ge substrate.**

Fig. S2. Typical volatile resistive switching in VO₂. I-V curve measured at 330K for one of the Au/VO₂/Ge devices.
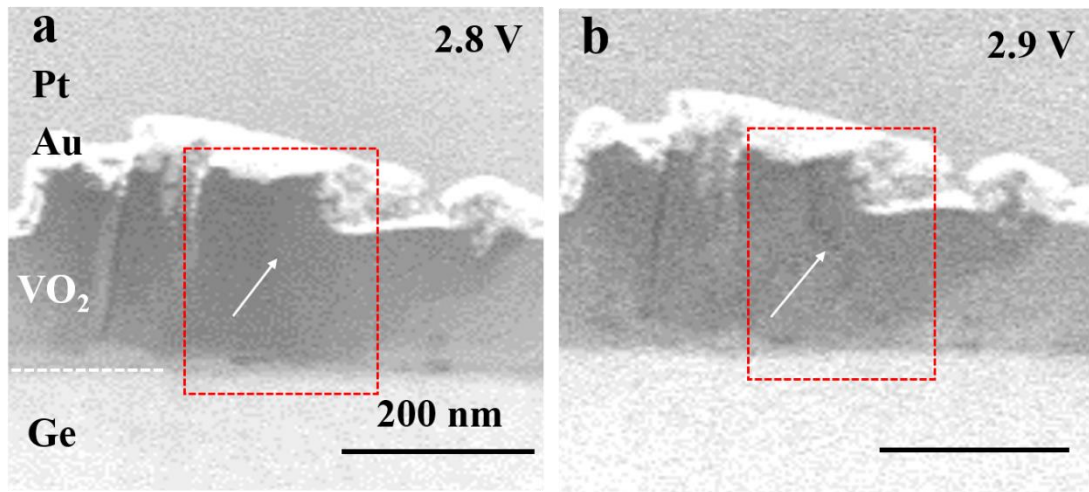

Fig. S3. (a) Before and (b) after the formation of the conductive filament. The position of the conductive filament is indicated by the white arrow.
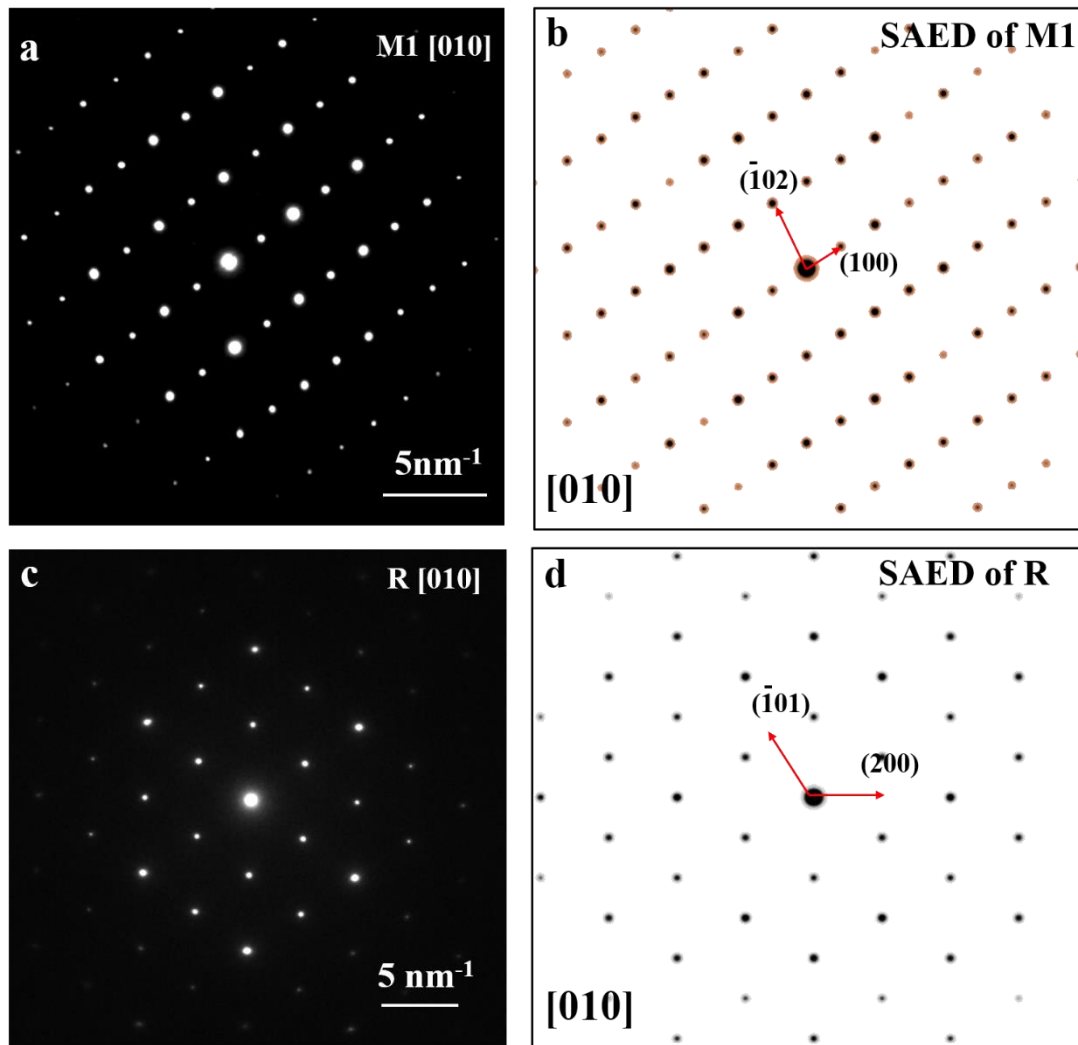
Fig. S4. The selected area electron diffraction analyses for VO₂. (**a**) The SAED pattern for M1 phase VO$_2$ at [010] zone axis. (**b**) Simulated M1 phase VO$_2$ from [010] direction. (**c**) The SAED for high temperature rutile phase VO$_2$ from [010] zone axis. (**d**) Simulated SAED for R phase VO$_2$ from the same zone axis.
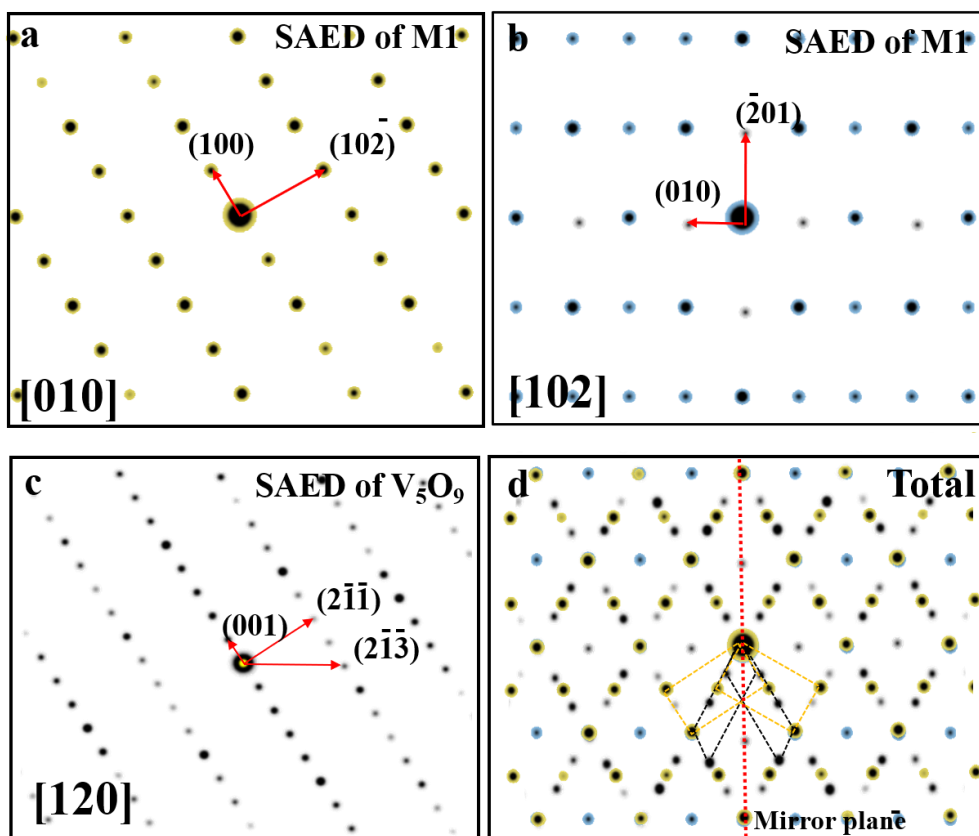
Fig. S5. Simulated electron diffraction patterns. **(a)**, **(b)**, **(c)**, Simulated electron diffraction patterns for M1 VO_2 from [010] and [102], and V_5O_9 from [120], respectively. **(d)** The combination of M1 VO_2 [102] diffraction, two sets of twinned V_5O_9 from [102] and M1 VO_2 from [010], which matches well with the experimental results shown in the main text. The mirror plane of twins is shown in red. The yellow parallelograms mark the base vectors for M1 VO_2 in reciprocal space, while the black parallelograms show those of V_5O_9.
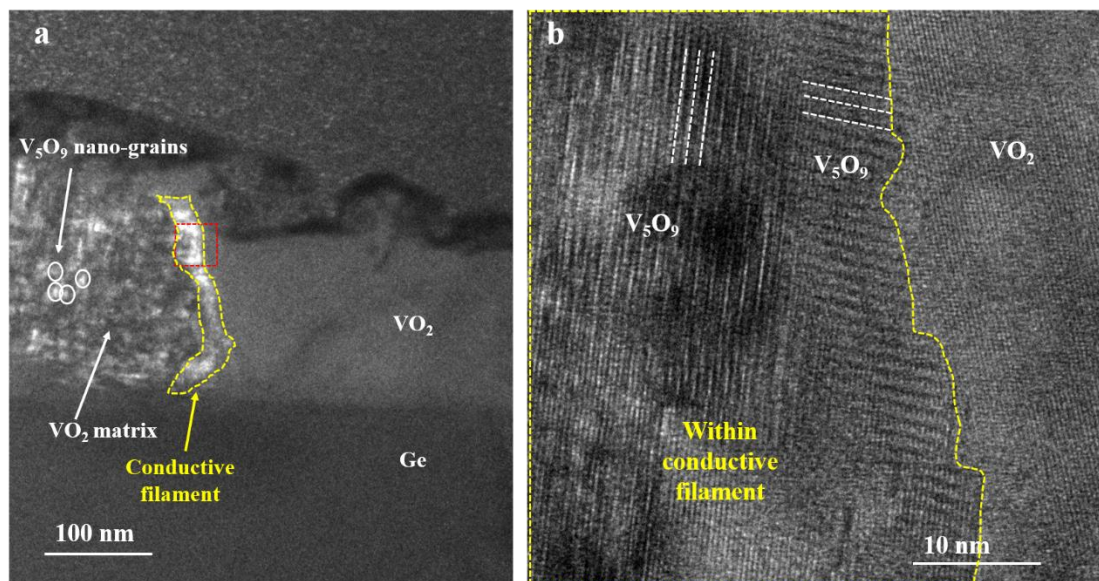
7

Fig. S6 TEM studies on the conductive filament area. (**a**) Dark field TEM images showing the V_5O_9 conductive filament (in yellow). Some V_5O_9 nano-grains within VO_2 matrix have been encircled. (**b**) High resolution TEM image acquired from the red rectangle area in (a), showing the twin structure of V_5O_9 phase.
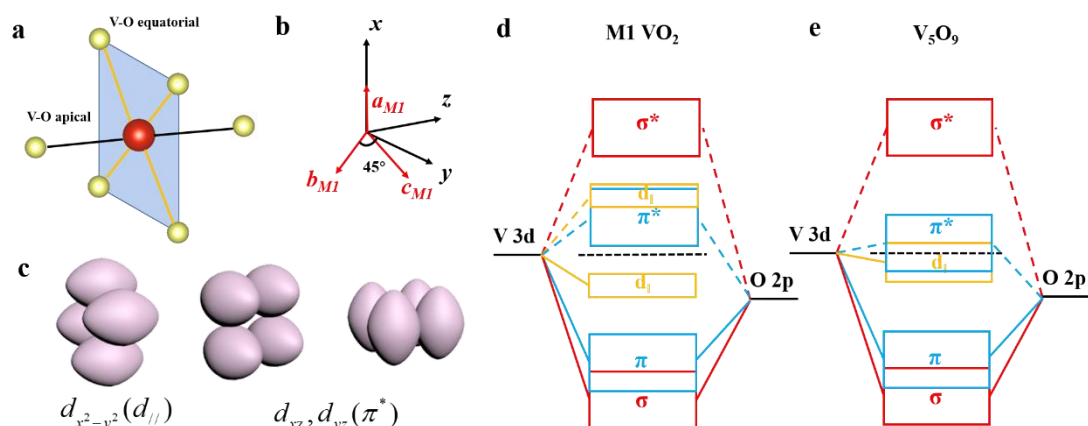

Fig. S7. Orbital hybridization analyses for two relevant vanadates. (**a**) Schematic diagram showing the VO_6 octahedron. The apical and equatorial V-O bonds are indicated in black and orange colors. (**b**) The relationship between the geometric axis (red arrows) and the coordination axis of M1 phase VO_2. (**c**) The illustration of

8

vanadium t_{2g} d orbitals. (**d**), (**e**) Schematic of the orbital band structure of M1 phase

VO_2 and V_5O_9 phase, deduced from the measured EELS result.
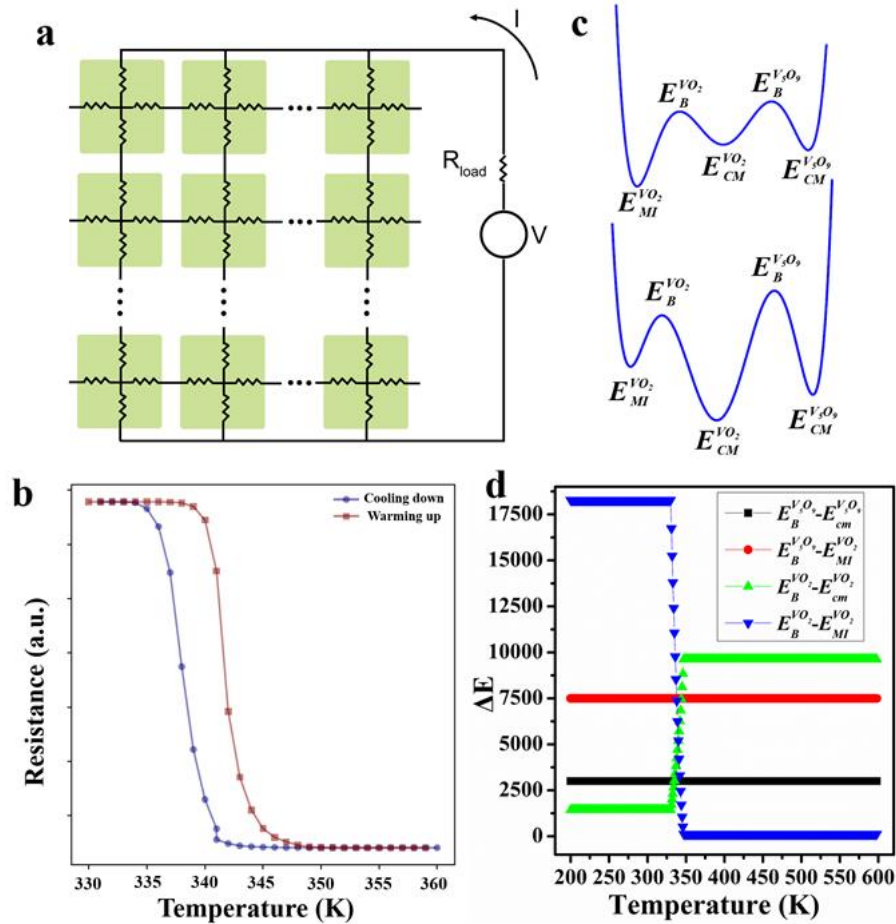

Fig. S8. Sketch representation of the Mott resistor network model. (**a**) The

simulation circuits. Each site of a grid of size $L \times W$ is represented by 4 resistors. All

resistors in each site have the same one of 3 possible values correspond to the 3 phases:

metal VO_2, metal V_5O_9 and insulator VO_2, respectively. (**b**) Simulated R-T curve for

VO_2 volatile switching. The transition temperature is about 340 K. (**c**) Cartoon

schematic of the free energy of the system near T_{IMT} ($T < T_{IMT}$ on the top and $T > T_{IMT}$ at

the bottom). (**d**) Energies vs Temperature computed as discussed in the Supporting
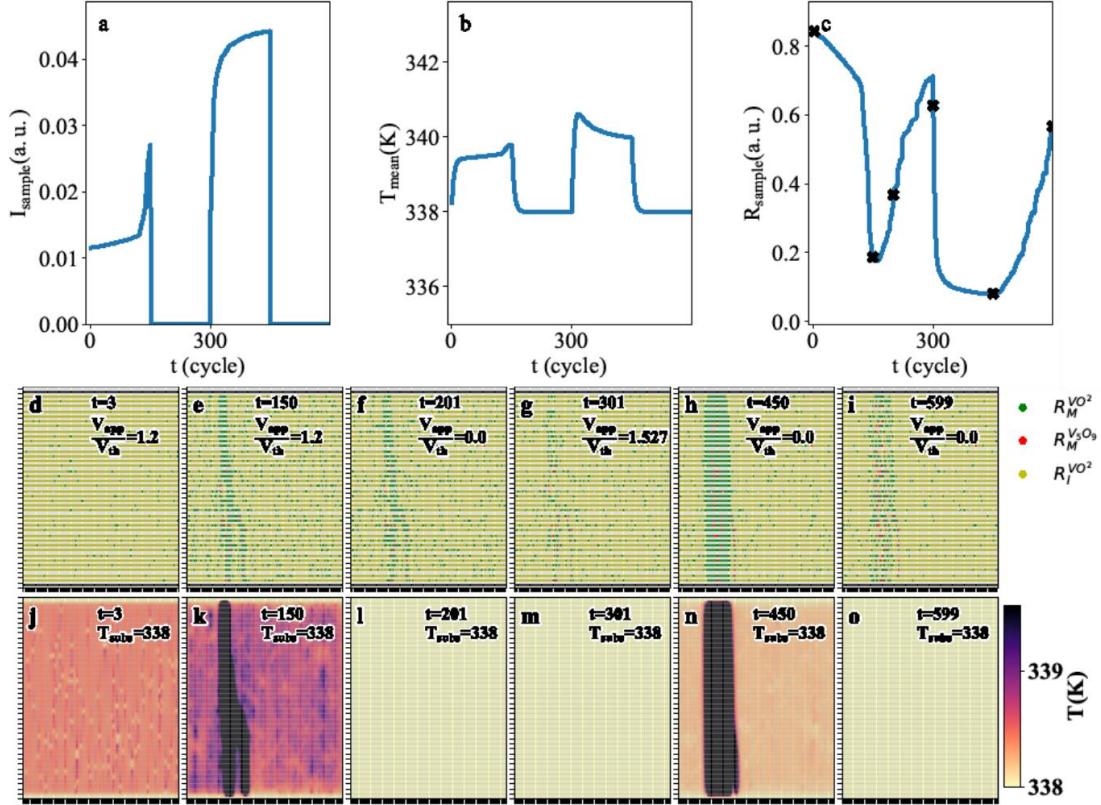
Information.

Fig. S9. Simulations of the formation and relaxation of volatile conductive filament at 338 K (close to IMT temperature). (**a**) Electric current of the system in arbitrary unit as a function of time. A first pulse voltage of V_{app}/V_{th}=1.2 is applied from t=1 until t=150 and a second pulse of V_{app}/V_{th}=1.527 is applied from t=300 until t=450. The substrate temperature is fixed at T=338 K. V_{th} is the voltage that triggers threshold switching. (**b**) Average temperature through the network as a function of time. The small variation in the sample temperature at 338 K is due to the Joule heating caused by applied voltage. (**c**) Resistance of the resistor network in arbitrary unit as a function of time. (**d**)-(**i**) Distributions of metallic rutile VO_2 (green), V_5O_9 phase (red) and insulator M1 VO_2 (yellow) at different time: (**d**) t=3 (starting of the first pulse of voltage

10

$V_{app}/V_{th}=1.2$); (**e**) t=150 (formation of volatile conductive filament. The conductive filament is formed of rutile VO_2); (**f**) t=201 (during the relaxation process); (**g**) t=301 (starting of the first pulse of voltage $V_{app}/V_{th}=1.527$); (**h**) t=450 (first snapshot after the second pulse); (**i**) t=599 (during the relaxation process). A stronger second pulse was applied on the sample and the conductive filament is largely formed by rutile VO_2 (Joule heating). Notably very small patches of V_5O_9 can be found. The t is the simulation step. (**j**)-(**o**) The corresponding temperature distributions in the unit of Kelvin. The full simulated movie can be found in the Supplementary Video 4.
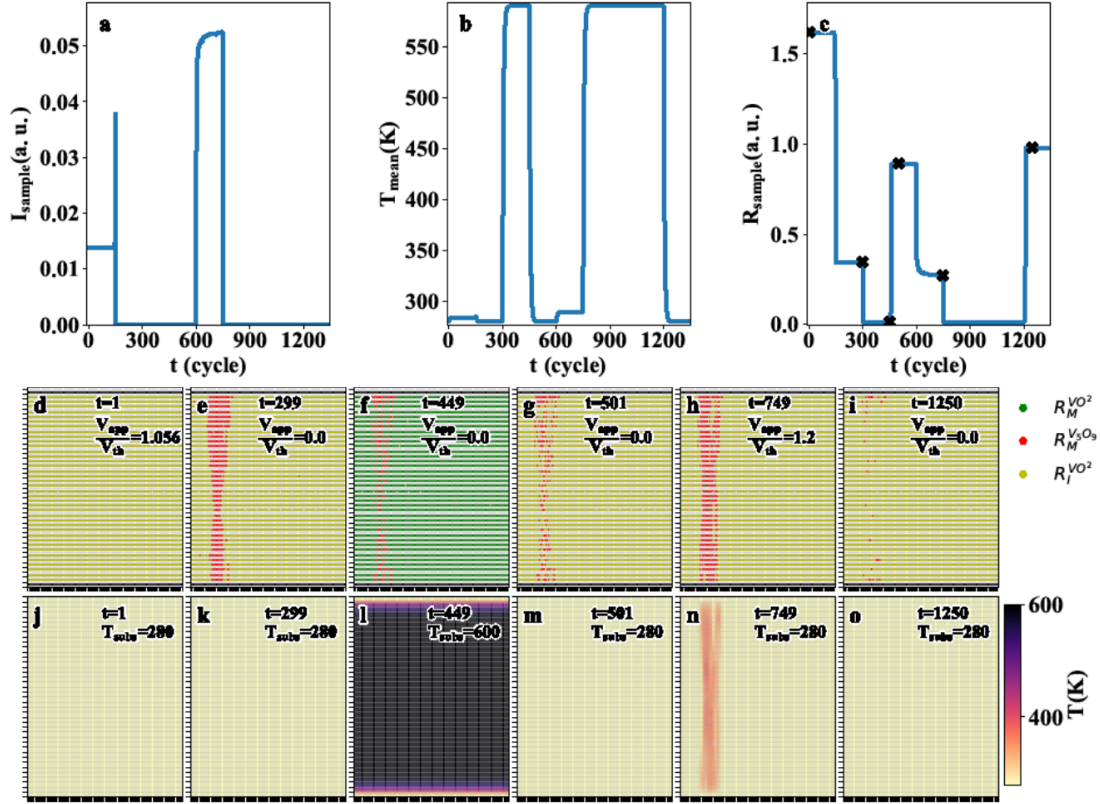
Fig. S10. Simulation results for non-volatile conductive filament at 280 K (far from IMT temperature). a, Current across the resistor network in arbitrary unit as a function of time. A first V_{app}/V_{th}=1.056 pulse is applied from t=1 to t=150 and a second one of V_{app}/V_{th}=1.2 from t=600 to t=750. **b,** Average temperature through the network as a function of time. The small variation in the sample temperature at 280 K is due to the applied voltage that induces Joule heating. The substrate is heated to 600 K for annealing at 300<t<450 and 750<t<1200. **c,** Resistance of the network in arbitrary unit as a function of time. **d-i**, Distribution of metallic rutile VO_2 (green), V_5O_9 phase (red) and insulator M1 VO_2 (yellow) at different time as indicated in **c** with star marks. **d,** t=1 (starting position); **e,** t=299 (after the relaxation of the first applied voltage V_{app}/V_{th}=1.056); **f,** t=449 (just before the finishing of the first annealing process); **g,** t=501 (after the relaxation of the first annealing process); **h,** t=749 (during the second

pulse of voltage $V_{app}/V_{th}=1.2$); **i,** t=1250 (during the relaxation of the last annealing process). Note, the t is the simulation step. **j-o**, The corresponding temperature distributions in the unit of Kelvin. The full simulated movie can be found in the Supplementary Video 5.
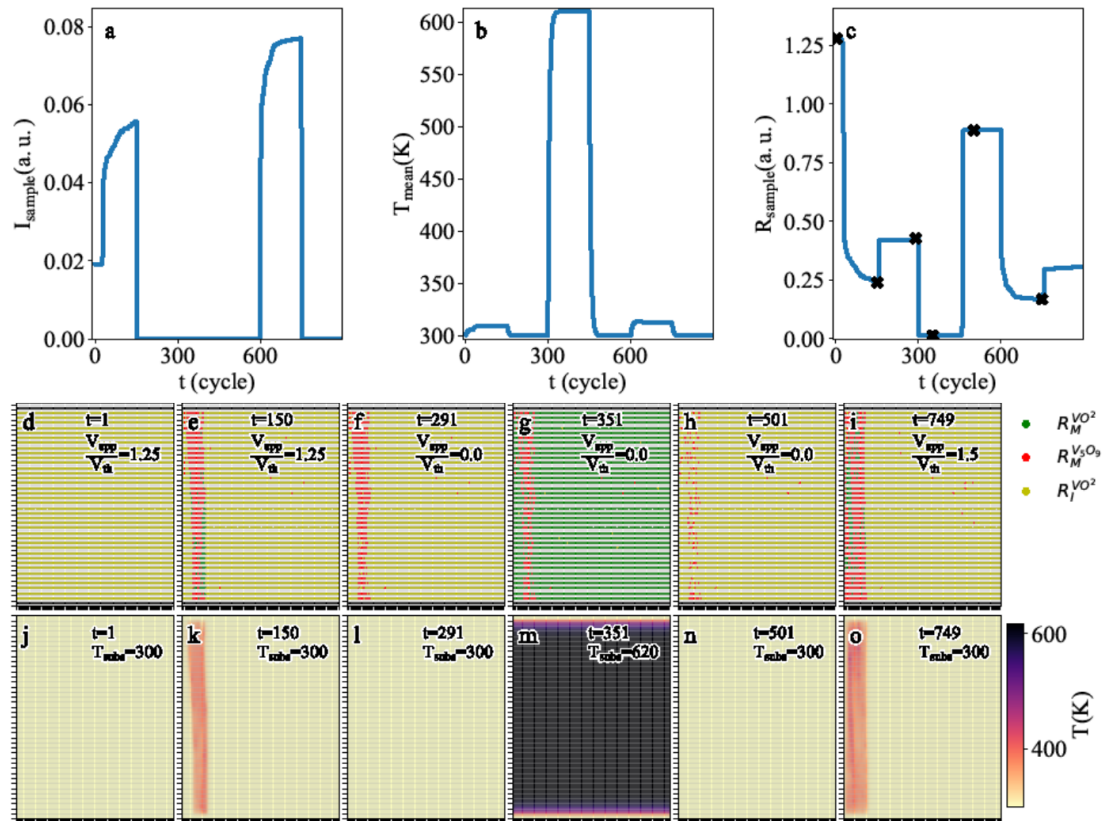

Fig. S11. Simulation for volatile and non-volatile conductive filament at room temperature. **a,** Current across network in arbitrary unit as a function of time. A first voltage $V_{app}/V_{th}=1.25$ pulse is applied from t=1 until t=150 and a second $V_{app}/V_{th}=1.5$ is applied from t=600 until t=750. **b,** Average temperature through the network as a function of time. The small variation in the temperature of the sample at 300 K is due to the applied voltage that induce Joule heating. The substrate temperature is increased up to 620 K for annealing purpose at $300<t<450$. **c,** Resistance of the network in

13

arbitrary unit as a function of time. **d-i,** Distribution of metallic rutile VO_2 (green), V_5O_9 phase (red) and insulator M1 VO_2 (yellow) at different times. **d,** t=1 (starting position); **e,** t=150 (during first pulse voltage of V_{app}/V_{th}=1.25 is applied); **f,** t=291 (after relaxation of the first pulse); **g,** t=351 (during the annealing process); **h,** t=501 (after the annealing process); **i,** t=749 (the second pulse with smaller stimuli). Notably, once the non-volatile V_5O_9 filament is formed the surrounding areas of the conductive filament might heated up by the stronger pulse, thus driving the VO_2 insulating phase into a metallic VO_2 via IMT. **j-o,** The corresponding temperature distributions in degrees Kelvin. The full simulated movie can be found in the Supplementary Video 6.
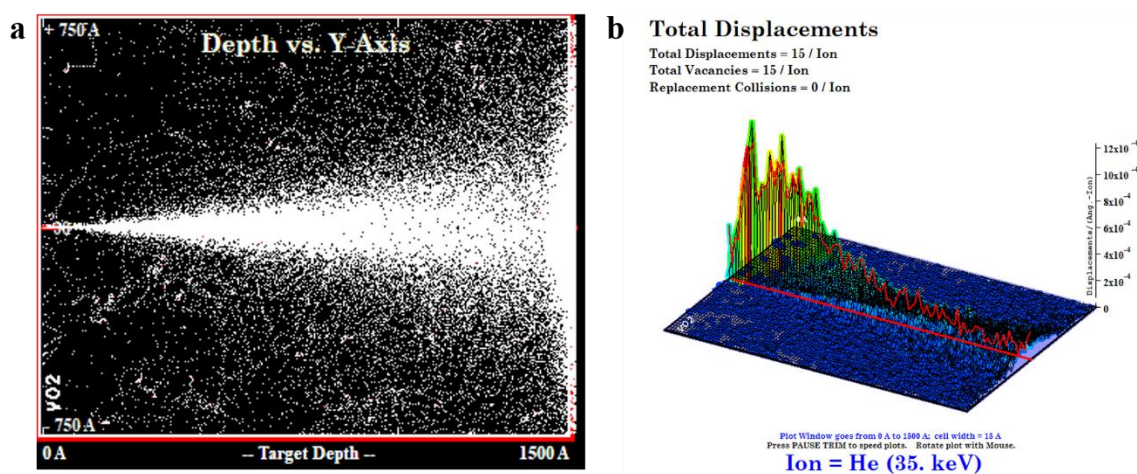

Fig. S12. Simulations on the He^+ ions injection into VO_2 film. a, Ion beam track for 35 keV He^+ ions incident on a film of 1500 Å of VO_2. Beam is incident from the left. **b**, Displacements in the VO_2 film as a function of depth. The track of displacements is narrow through the film.

Supplementary Video 1 | *In-situ* TEM observation of the V_5O_9 conductive filament.

Supplementary Video 2 | V₅O₉ conductive filament reappear at the same location after the annealing.

Supplementary Video 3 | The whole time dependent numerical simulations for Fig. 5.

Supplementary Video 4 | The whole time dependent numerical simulations for Supplementary Materials Fig. 9.

Supplementary Video 5 | The whole time dependent numerical simulations for Supplementary Materials Fig. 10.

Supplementary Video 6 | The whole time dependent numerical simulations for Supplementary Materials Fig. 11.

1. J. D. Valle, P. Salev, F. Tesler, N. M. Vargas, Y. Kalcheim, P. Wang, J. Trastoy, M.-H. Lee, G. Kassabian, J. G. Ramírez, M. J. Rozenberg, I. K. Schuller, Subthreshold firing in mott nanodevices. *Nature*, **569**, 388–392 (2019).

2. P. Stoliar, J. Tranchant, B. Corraze, E. Janod, M. -P. Besland, F. Tesler, M. Rozenberg, L. Cario. A leaky-integrate-and-fire neuron analog realized with a mott insulator. *Adv. Funct. Mater.*, **27**, 1604740 (2017).

3. S. A. Cybart, E. Y. Cho, T. J. Wong, B. H. Wehlin, M. K. Ma, C. Huynh, R. C. Dynes, Nano Josephson superconducting tunnel junctions in $YBa_2Cu_3O_{7-\delta}$ directly patterned with a focused helium ion beam. *Nat. Nano.* **10**, 598-602 (2015)